Petroleum Science 20 (2023) 3687–3699

Contents lists available at ScienceDirect

Petroleum Science

journal homepage: www.keaipublishing.com/en/journals/petroleum-science

Original Paper

Experimental study of the temporary plugging capability of diverters to block hydraulic fractures in high-temperature geothermal reservoirs

Dao-Bing Wang [a], Hao Qin [b], Yong-Liang Wang [c], Jian-Qiao Hu [d], Dong-Liang Sun [a, *], Bo Yu [a, **]

[a] School of Mechanical Engineering, Beijing Institute of Petrochemical Technology, Beijing, 102617, China
[b] Jinan Branch, China Petroleum and Chemical Corporation, Jinan, 250101, Shandong, China
[c] School of Mechanics and Civil Engineering, China University of Mining and Technology (Beijing), Beijing, 100083, China
[d] LNM, Institute of Mechanics, Chinese Academy of Sciences, Beijing, 100190, China

ARTICLE INFO

Article history:
Received 4 January 2023
Received in revised form
20 March 2023
Accepted 2 July 2023
Available online 3 July 2023

Edited by Jia-Jia Fei

Keywords:
High temperature
Diverter material
Fracture plugging capability
Hydraulic fracturing
Experimental study

ABSTRACT

The effective plugging of artificial fractures is key to the success of temporary plugging and diverting fracturing technology, which is one of the most promising ways to improve the heat recovery efficiency of hot dry rock. At present, how temporary plugging agents plug artificial fractures under high temperature remains unclear. In this paper, by establishing an improved experimental system for the evaluation of temporary plugging performance at high temperature, we clarified the effects of high temperature, injection rate, and fracture width on the pressure response and plugging efficiency of the fracture. The results revealed that the temporary plugging process of artificial fractures in hot dry rock can be divided into four main stages: the initial stage of temporary plugging, the bridging stage of the particles, the plugging formation stage, and the high-pressure dense plugging stage. As the temperature increases, the distribution distance of the temporary plugging agent, the number of pressure fluctuations, and the time required for crack plugging increases. Particularly, when the temperature increases by 100 °C, the complete plugging time increases by 90.7%.

1. Introduction

Geothermal energy is a type of high-quality renewable energy that is clean, safe, and low-carbon; it is also abundantly available and widely distributed. The development and utilization of geothermal energy offer the advantages of a continuous and stable energy supply, efficient recycling, and regeneration. It can not only reduce greenhouse gas emissions but also improve the ecological environment (Geothermal Energy, 2013). Geothermal energy has become the focus of new clean energy research and development. It can contribute new kinetic energy to the structural transformation of China's energy landscape.

Due to the low permeability of the hot dry rock, the technologies of hydraulic fracturing and more extensive and complex artificial fracture network formation are needed to enhance thermal energy extraction capacity (Fehler, 1989; Kumari et al., 2018; Shi et al., 2013; Zhang et al., 2019; Ghassemi, 2012; Evans et al., 1999). A complex fracture system is generated during the hydraulic fracturing process so that the underground has a larger heat exchange area. Studies have shown that increasing the number and complexity of artificial fractures is conducive to improving the permeability and heat transfer area of hot dry rock and can greatly improve heat recovery efficiency (Evans et al., 1999; Fehler, 1989; Wang et al., 2021).

At present, conventional hydraulic fracturing is a common method for creating artificial fracture systems underground. However, conditions such as great burial depth, high temperatures, and strong stress anisotropy limit conventional hydraulic fracturing technology's usefulness when forming a complex fracture network (Zhou et al., 2009; Wang, 2017). To overcome this problem,

* Corresponding author.
** Corresponding author.
E-mail addresses: sundongliang@bipt.edu.cn (D.-L. Sun), yubobox@vip.163.com (B. Yu).

https://doi.org/10.1016/j.petsci.2023.07.002

temporary plugging and diverting fracturing technology can be used (Liang et al., 2018; Zhou et al., 2022). During the fracturing process, temporary plugging agents are used to temporarily plug the created fractures, thereby increasing the net pressure in the fractures. This pressure increase can force fracture diversion and thus improve fracture complexity (Potapenko et al., 2009). Effective temporary plugging of fractures and increased pressure in fractures are vital during this process of temporary plugging and diverting fracturing (Wang et al., 2015a, 2015b, 2020).

To capture the plugging performance of temporary plugging agents, scholars have carried out many experimental studies (Wang, 2017) using different types of temporary plugging agents and considering various factors influencing plugging characteristics (Smith et al., 1969; Calçada et al., 2015; Evans et al., 1999; Yuan et al., 2020; Zhou et al., 2022). In terms of the types of temporary plugging agents used, the most common diverter materials are the fiber type, particle type, and mixed type. Experimental studies (Droger et al., 2014; Potapenko et al., 2009; Shi et al., 2013; Zhou et al., 2009) have shown that the fiber-type temporary plugging agent has good plugging performance in various reservoirs, such as carbonate rock, shale gas, and tight sandstone. After fibers enter a fracture, the net pressure within the fracture increases significantly. Li et al. (2018) added a fibrous temporary plugging agent to mixed materials to form a water-based temporary plugging diverter fluid. They then tested its plugging performance in a fracture slot with a 2 mm opening. The results showed that the fiber-type temporary plugging agent had effective sealing and plugging performance in fractures. Other scholars have evaluated the plugging performance of degradable fibers through laboratory experiments. These experiments have demonstrated that increasing pressure can make a fiber-based temporary plugging agent more quickly form a plugging zone in fractures. As the injection rate increases, the net pressure in the fracture becomes higher and the filtration rate of the fluid carried by the temporary plugging agent is faster. Therefore, it is easier to block fractures effectively and temporarily with increased pressure and higher fiber concentration.

In recent years, granular temporary plugging agents, which can change shape with temperature, have been applied during the process of temporary plugging and fracturing. The experimental results (Mansour et al., 2017) show that as particles expand and bridging plugging begins, the fluid filtration in the fracture decreases to zero and the net pressure in the fracture increases gradually. This suggests that the plugging effect of temporary particle plugging is very strong, and the plugging section of the fracture can withstand very high pressure. The particle size distribution of the granular temporary plugging agent also affects the plugging effect. During the initial stage, a temporary plugging agent with a large particle size plays an important role in plugging large fractures. Then a temporary plugging agent with a small particle size begins to fill in the gap to achieve a good plugging effect (Mansour et al., 2017; Allison et al., 2011). Particularly, Alsaba et al. (2017, 2014) proposed a new selection criterion of particle size for the granular temporary plugging agents and determined how to plug fractures with this criterion. Some scholars have sought to clarify whether the plugging effect is stronger when fiber-type and particle-type temporary plugging agents are mixed rather than unadulterated. The experimental results (Li et al., 2019; Xue et al., 2015) show that better plugging performance can be obtained by injecting a granular temporary plugging agent after injecting fiber. The larger particles first bridge at the narrow fracture mouth, and then the smaller fiber closes the gap in the bridging section. The recommended ratio of injected particle to fiber is 1:1.

Some scholars have experimentally studied the factors influencing plugging efficiency. These factors include the temporary plugging agent concentration, fiber–particle mixing ratio, fiber length, particle size, injection rate, and filter cake permeability. The experimental results (Liu, 2017) showed that increased fiber concentration can speed up fracture plugging and that the temporary plugging efficiency is better when there is a high fiber concentration. However, the temporary plugging efficiency of particles is opposite to that of fibers. When the particle concentration exceeds a certain level, the plugging rate decreases, and the plugging ability worsens. The fiber plugging efficiency is enhanced when the injection rate is relatively low, the fracture width is small, and the viscosity is high (Wang et al., 2015b). In addition, with increases in fiber length, concentration, and injection rate, the plugging efficiency of a temporary plugging agent on fractures can be improved (Fehler, 1989; Zhang et al., 2019; Van Domelen, 2017; Calçada et al., 2015). Based on the original method of temporary plugging and diversion, Van Domelen (2017) proposed strategies for improving the plugging effect, such as selecting a suitable carrier fluid, identifying a reasonable particle size distribution of the temporary plugging agent, and determining the correct injection process for the temporary plugging agent. The experimental result (Xue et al., 2015) show that the temporary plugging agent could effectively plug the fractures by means of bridge plugging, and the plugging strength reached 40 MPa.

Based on this literature review, the existing study focuses on the process of temporary plugging and diverting fracturing in oil and gas reservoirs, and experiments are mainly carried out under normal temperature conditions. However, unlike oil and gas reservoirs, hot dry rocks are mostly granite or tight metamorphic rocks with high temperatures. There are obvious differences in physical and mechanical properties. At the high-temperature environment, the temporary plugging agent experiences three mechanical states successively: the glass state, high elastic state, and viscous flow state (Ghassemi, 2012; Wang et al., 2023; Zhang and Zhao, 2019; Zheng et al., 2023). Eventually, creep behavior occurs at this high temperature, and properties such as pressure-bearing capacity and the elastic modulus change. Experiments showed that the elastic modulus of the temporary plugging agent changes by about 5% for every 1 °C change in temperature. The temporary plugging agent is deformed at the high temperature and its flow characteristics are changed. Therefore, the plugging performance is quite different at the high temperature, and the temporary plugging characteristics change significantly in hot dry rock. This difference due to the variation of temperature motivated us to investigate the plugging mechanism of diverter materials in artificial fractures at different temperatures.

2. Preparation of artificial fractures in hot dry rock

2.1. Expansion-induced cracking experiment

In this study, the expansion-induced cracking experiment was used to prepare the fractures required for exploring the temporary plugging characteristics of such fractures in hot dry rock. As shown in Fig. 1(a), the hot dry rock expansion-induced cracking device includes a frame body and a core limiting structure. This experimental device was designed by the Beijing Institute of Petrochemical Technology. The core limiting structure includes two semi-circular thick-walled cylinders and upper and lower backing plates. It is used to mimic the surrounding in-situ stress on the core during expansion-induced cracking experiments. The gap between each thick-walled cylinder and the core is surrounded by copper skin to ensure that the surface pressure on the core wall is even.

A core of Miluo granite outcrop from Hunan Province in southern China was selected for the experiment. A rock sample with a diameter of 107.5 mm and a height of 130 mm was drilled on the bulk granite. A through hole with a diameter of 16 mm was

Fig. 1. Hot dry rock expansion-induced cracking experimental device and sample. (**a**) Expansion-induced cracking device; and (**b**) hot dry rock sample.

drilled at the center of the sample to ensure that the drilled hole ran through the center of the core and was parallel to the height of the wall, as shown in Fig. 1(b). We measured the minimum diameter of the prepared core and calculated the difference from the core to the inner diameter of each thick-walled cylinder to determine the number of copper skins required to be wrapped outside the core. The core was wrapped with red copper skin, fixed by rubber bands, and placed on the bottom plate of the core limiting structure. Then the core and the outer wall of the copper skin were fixed with the two semi-circular thick-walled cylinders, and the thick-walled cylinders were connected with screws.

An HSCA-I type high-efficiency expansion agent was selected to carry out the expansion-induced cracking experiment. We mixed water and the expansion agent in a mass ratio of 1–3.6 as required and formed a mixed expansion agent after thorough stirring. The prepared mixed expansion agent slurry was injected into the core hole. The axial loading screw was twisted to make the upper backing plate contact the upper-end face of the core, and specific axial stress was applied for 48 h.

After the core was fractured, the upper backing plate and the two semi-circular thick-walled cylinders were opened, and the core was taken out. The fracture pattern of the core is shown in Fig. 2. The relatively complete internal crack structure after cracking was selected for subsequent 3D scanning.

2.2. Preparation of artificial fracture model

In order to repeat the experiment on temporary plugging characteristics with the same fracture shape, an artificial fracture model was made using 3D scanning and 3D printing technology. The fracture surface obtained from the expansion-induced cracking experiment was scanned with a HandySCAN3D 3D scanner, which has a scanning accuracy of 0.025 mm. Due to the irregular shape of the rock sample, the 3D scanning area of the fracture surface was smaller than that of the original fracture surface. The grid information of the fracture surface was generated and stored in a computer. To meet the high-temperature and high-pressure conditions required for exploring the temporary plugging characteristics of artificial fractures in hot dry rock at high temperatures, stainless steel material was selected as the 3D printing material. The material parameters are shown in Table 1. Based on the fracture

Table 1
Stainless steel material properties.

Property	Value
Yield point	470 N/mm^2
Tensile strength	570 N/mm^2
Elongation	>15%
Elastic modulus	2×10^5 N/mm^2
Thermal conductivity	15 W/(m·K)
Hardness	20 HRC

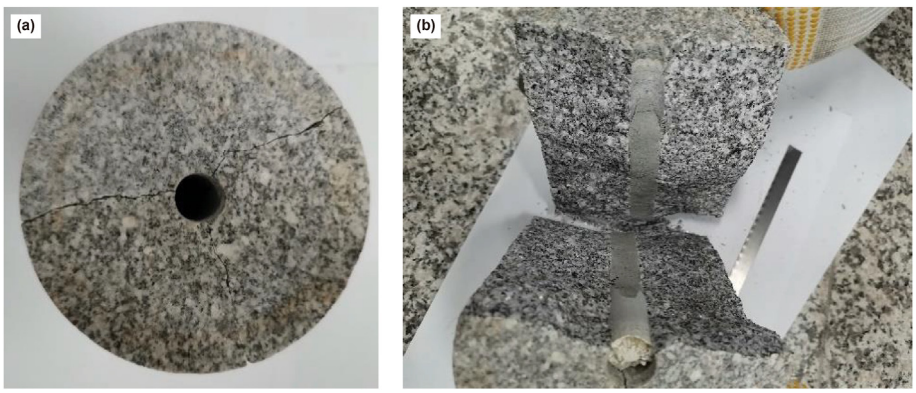

Fig. 2. Expansion-induced crack network structure at room temperature. (**a**) Upper bottom surface; and (**b**) fracture surface morphology.

mesh data, an EOS M 290 3D printer (Fig. 3(a)) was selected for printing the artificial fracture model.

After 3D scanning, the elevations of the upper and lower surfaces of the fracture are a function of the abscissa x and the ordinate y, which are denoted as h_1 (x, y) and h_2 (x, y), respectively. The fracture width $w(x, y)$ at any point (x, y) in the fracture is:

$$w(x,y) = h_2(x,y) - h_1(x,y) \quad (1)$$

As shown in Fig. 3(b) and (c), the fracture face created by the printer was rough. To prevent the temporary plugging agent from being blocked at the fracture inlet and allow it to smoothly enter the fracture during the experiment, the inlet was processed into a wedge shape during the printing process of the fracture model. The fracture model was divided into upper and lower parts, and the two parts of the fracture model were completely overlapped. The fracture length is 180 mm, the width is 38 mm, and the height of the overlapped upper and lower parts is 18 mm. We did not consider the fluid seepage at the fracture surface because the fracture model was not permeable.

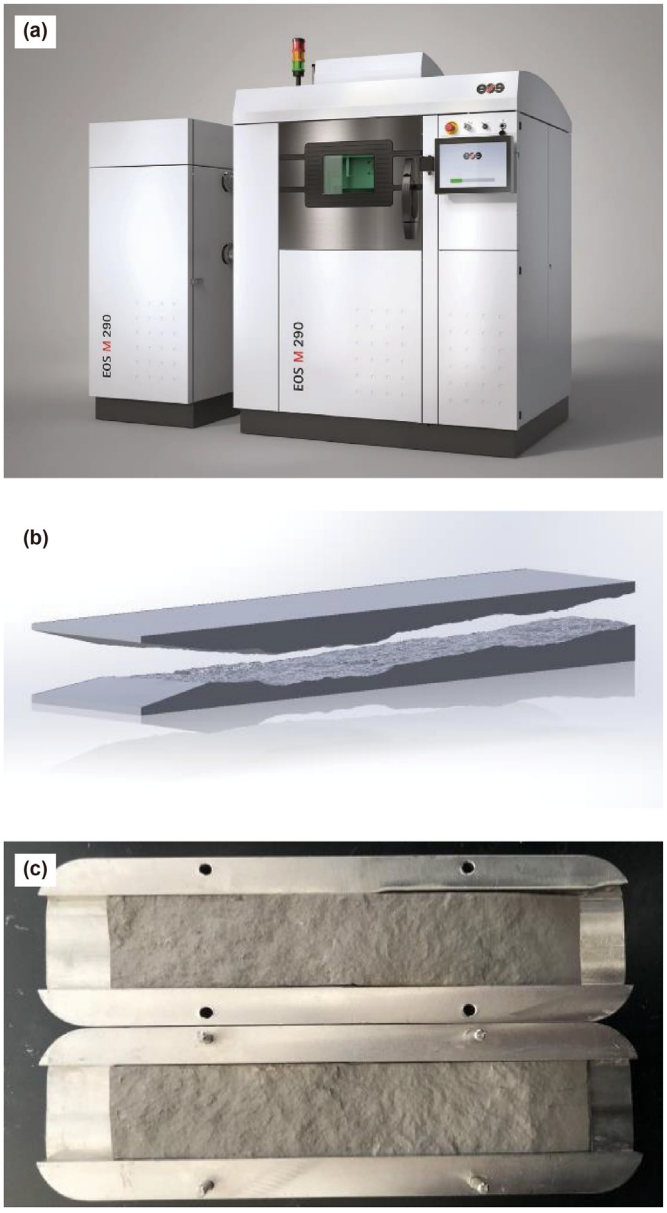

Fig. 3. Artificial fracture model of hot dry rock. (**a**) EOS M 290 3D printer; (**b**) 3D-scanned fracture surface structure; and (**c**) 3D-printed artificial fracture model.

3. Experimental setup and material preparation

3.1. Experimental device

To determine the temporary plugging characteristics of artificial fractures in hot dry rock, we developed an experimental system for evaluating temporary plugging performance at high temperatures. Fig. 4 illustrates the flow chart of the experimental system for evaluating temporary plugging performance at high temperature. This system is an improved version of the original experimental system for investigating the temporary plugging of fractures. Its main components are an artificial fracture model, metal rock slab, fracture clamping unit, confining pressure loader, liquid injection pump, confining pressure pump, container, data acquisition system, pressure sensor, control valve, and temperature control system. High-pressure pipelines are used to connect the various components of the system.

Particularly, the temperature control system is mainly composed of a heating unit and a temperature control unit, both of which are installed outside the fracture clamping unit to simulate the high-temperature environment of hot dry rock. The maximum temperature is 200 °C. The temperature sensor is in contact with the fracture wall through the outer small hole. At the same time, the temperature control unit is equipped with a real-time temperature display system, so the effect of real-time viewing of the heating temperature can be achieved during the experiment. The carrier liquid of the temporary plugging agent is injected at room temperature, which is not consistent with the design temperature, which is the same as the actual situation of the oilfield field engineering.

The confining pressure pump and the confining pressure loader constitute the experimental confining pressure system. The maximum pump speed of the confining pressure pump is 100 mL/min, and the maximum confining pressure is 70 MPa. The pressure sensor is used to record the pressure change in the temporary plugging joint. The temporary plugging agent is contained in an intermediate container with a maximum volume of 10 L, one end of which is connected to the liquid injection pump, and the outlet is connected to the fracture clamping unit. The fracture clamping unit with the artificial fracture model and heating unit is placed above the confining pressure loader and consists of a diversion cavity, upper and lower pistons, and liquid inlet and outlet interfaces. The

Fig. 4. Experimental system for evaluating temporary plugging performance of high-temperature fractures in hot dry rock.

outlet end is connected to a collector for collecting waste liquid. The data acquisition interval is 0.1 min.

During the experiment, the prepared temporary plugging agent slurry was first poured into the container. Then the artificial fracture model was installed in the metal slate and placed in the center of the fracture clamping unit. The inner metal slate was fixed by the pistons at both ends, and the heating unit was installed outside. After connecting the high-pressure pipeline, the clamping unit was placed on the confining pressure loading table and preloaded by manually turning the screw. Then we set the target confining pressure and applied the confining pressure to the fracture to mimic the in-situ stress during the actual temporary plugging construction. The fracture was heated to the target temperature by setting the temperature control unit. After the target temperature was reached, the corresponding temporary plugging agent injection rate and experimental protection pressure limit value were set. Subsequently, the pre-prepared distilled water was injected into the bottom of the piston of the container through the liquid injection pump, and the piston was pushed upward so that the temporary plugging agent slurry entered the high-pressure pipeline and eventually reached the artificial fracture in the fracture-holding unit. The pressure sensor recorded the pressure change in the fracture during the plugging process. When the pressure reached the pressure limit value, the liquid injection was stopped and the experiment was ended. After cooling, the artificial fracture model was taken out.

3.2. Material preparation

Temporary plugging agents are widely used in temporary plugging and diversion fracturing, and copolymers of lactic acid and glycolic acid are usually used to produce various types of temporary plugging materials, such as particles, powders, and fibers. To mimic the plugging process under the high-temperature environment of hot dry rock reservoirs, we selected two high-temperature-resistant degradable temporary plugging agents for mixing. Fig. 5(a) shows a cylindrical particle with a diameter of 3 mm and a length of 3 mm; its density is about 1.26 g/cm^3. Fig. 5(b) shows a 40-mesh fiber powder.

As part of the experiment, the mixed particle and fiber powder temporary plugging agent needed to be carried by the fracturing fluid to flow in the high-pressure pipeline. To avoid the rapid settlement of the temporary plugging agent in the intermediate container and high-pressure pipeline, 0.3 wt% hydroxypropyl guar gum, 0.02 wt% citric acid, 0.15 wt% cross-linking regulator, and 0.3 wt% cross-linking agent were mixed with water to create a high-viscosity fracturing fluid (Fig. 6). Among the components, guar gum and citric acid were used to adjust the viscosity and pH value of the fracturing fluid, respectively. The viscosity of the carrier fluid is equal to 50 mPa·s at room temperature without cross linker. After adding the crosslinking agent, the fluid viscosity is more than 100 mPa·s.

6 L of water was put in a measuring cylinder and stirred at the rotation speed of 1500 rpm to prepare the fracturing fluid. An electronic balance was used an electronic balance to weigh 1.2 g of citric acid, which is poured into the water slowly, and stirred for 2 min. 18 g of guar gum was weighed, and was slowly poured into the water, and stirred for 30 min. Then 9 g of the cross-linking regulator was weighed, and poured into the water slowly, and the weighed 18 g of the cross-linking agent was poured into the mixture and stirred. After the fracturing fluid is prepared, 30 g of 3 mm particles and 90 g of 40-mesh fiber powder were weighed and poured into the fracturing fluid and stirred to obtain the required temporary plugging agent solution.

3.3. Experimental procedure

This paper experimentally investigates the effects of high temperature, injection rate, and fracture width on the temporary plugging characteristics of artificial fractures in hot dry rock (see Table 2). The main experimental scheme is as follows:

(1) Effect of high temperature

To study the effect of high temperature on the temporary plugging characteristics of hot dry rock reservoirs, a composite temporary plugging scheme of particles and fiber powder was adopted in the experiment. First, we mixed the diverter and the fracturing fluids to form the plugging agent solution. Then we fixed the installation. The artificial crack width in the metal slate was set to 4 mm using shims of different thicknesses. The target confining pressure was set to 20 MPa, and the confining pressure was loaded to prevent the fracture width from increasing due to excessive pressure. The experimental displacement was set to 50 mL/min. The target temperatures were 25, 50, 100, and 150 °C. Temporary plugging experiments were carried out at each temperature.

Fig. 5. High-temperature-resistant particle and fiber powder temporary plugging agent. (**a**) Particles; and (**b**) fiber powder.

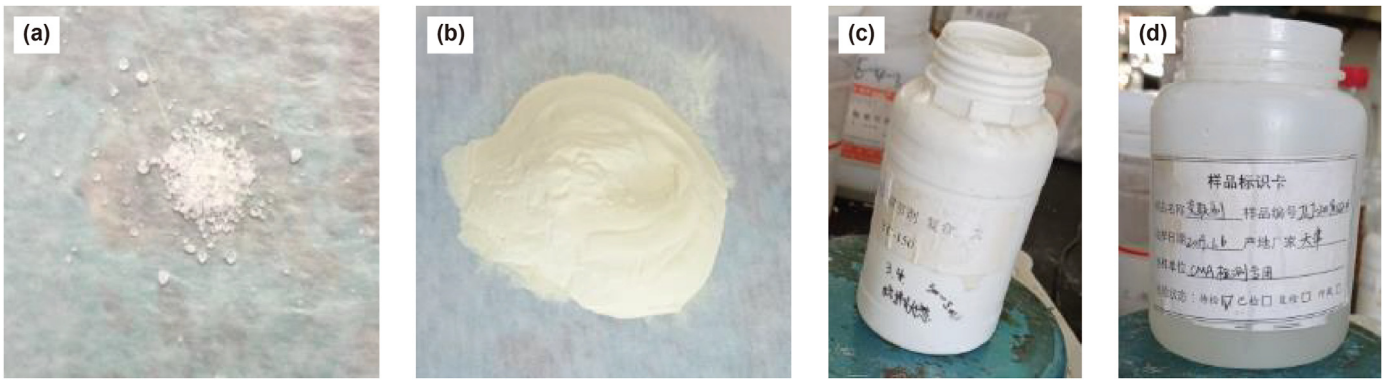

Fig. 6. Experimental material of high-viscosity fracturing fluid configuration. (**a**) Citric acid; (**b**) guar gum; (**c**) cross-linking regulator; and (**d**) cross-linking agent.

Table 2
Experiment-related attribute parameters.

Property	Value
3 mm particle	0.5% g/mL
40-mesh fiber powder	1.5% g/mL
Citric acid	0.02 wt%
Guar gum	0.3 wt%
Cross-linking regulator	0.15 wt%
Cross-linking agent	0.3 wt%
Water	6 L
Confining pressure	20 MPa
Injection rate	30/50/70 mL/min
Fracture width	4/5/6 mm
Temperature	25/50/100/150 °C

During each experiment, the experimental pressure, liquid output, and experimental time were recorded.

(2) Effect of injection rate

To study the effect of the temporary plugging agent injection rate on temporary plugging characteristics under high temperature, the same temporary plugging agent proportioning scheme as in (1) was used to configure 6 L of temporary plugging agent. The fracture width was fixed to 4 mm using shims of different thicknesses. The confining pressure was set to 20 MPa, and the experimental temperature was set to 100 °C. After heating to the target temperature, temporary plugging experiments were carried out using the injection rates of 30, 50, and 70 mL/min, respectively. During each experiment, the experimental pressure, liquid output, and experimental time were recorded.

(3) Effect of fracture width

In order to study the effect of fracture width on temporary plugging characteristics under high temperature, the same temporary plugging agent proportioning scheme as in (1) and (2) was used to configure 6 L of temporary plugging agent. The confining pressure was set to 20 MPa, the injection rate was set to 50 mL/min, and the experimental temperature was set to 100 °C. After heating to the target temperature, the fracture widths were adjusted to 4, 5, and 6 mm using gaskets of different thicknesses, respectively. Temporary plugging experiments were carried out at different fracture widths. During each experiment, the experimental pressure, liquid output, and experimental time were recorded.

4. Experimental results

4.1. Effect of high temperature on temporary plugging characteristics

(1) Plugging process

Because hot dry rock is located in a high-temperature environment, the temperature has an important impact on the rheology of the carrier fluid and the plugging ability of the temporary plugging agent. In particular, high temperatures reduce the viscosity of the carrier fluid. When the temporary plugging agent enters the artificial fracture of the hot dry rock with the carrier fluid, it undergoes a lengthy transportation process in the fracture. As the temperature gradually increases, the velocity of the carrier fluid in the fracture also increases. After the temporary plugging agent bridges the fracture, the impact strength of the fluid on the temporary plugging body continues to increase. This causes some temporary plugging agents to leave the original sealing position and flow to the far end of the fracture, indicating that the plugging position of the temporary plugging agent should be changed.

To explore the influence of temperature on the plugging position of the temporary plugging agent in the process of temporary plugging and fracturing, we designed the experiment at three different temperatures: 50, 100, and 150 °C. In the experiment's temporary plugging scheme, a temporary plugging agent comprised of 3 mm particles and 40-mesh fiber powder was used to block fractures that are 4 mm each in width. The experimental results show that because the particle size of the temporary plugging agent was matched with the fracture width, the plugging of artificial fractures by the temporary plugging agent was concentrated in the front of each fracture.

In the process of temporarily plugging artificial fractures, we identified four main stages, as shown in Fig. 7. The first stage was temporary plugging. During this stage, the temporary plugging agent particles had not formed a bridge in the fracture. The particles and fiber powder entered the artificial fracture with the carrier fluid and then were discharged from the fracture outlet. At the end of this stage, only a small amount of the granular temporary plugging agent was left in the fracture.

As the temporary plugging experiment continued, it entered the second stage; that is, the initial bridging stage of the particles. Most of the temporary plugging agents discharged through the fracture outlet in this process were fiber powder agglomerates. The amount of granular temporary plugging agent decreased, and the discharge

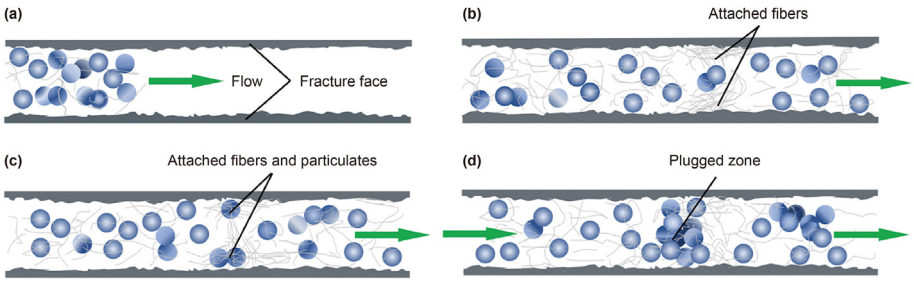

Fig. 7. Schematic diagram of four stages of temporary plugging in fractures. (**a**) Initial stage of temporary plugging; (**b**) the initial stage of particle bridging; (**c**) the particle-capturing fiber powder agglomerate formation plugging stage; and (**d**) high-pressure compaction plugging stage.

rate at the outlet showed a downward trend.

Then the plugging process entered the third stage, in which particles captured fiber powder agglomerates to form plugging bodies. Due to the limitation of fracture width, the granular temporary plugging agent that entered the artificial fracture through the high-pressure pipeline continued to bridge the front end of the fracture. The distribution density of the diverter increased gradually, and the flowable area of the fluid decreased. This caused both the particulate temporary plugging agent and the fiber powder in the carrier fluid flowing through the front of the fracture to be captured and form a plugging zone. At this time, the fluid pressure in the fracture gradually increased.

Finally, the temporary plugging process entered the fourth stage; namely, the high-pressure dense plugging stage. During this stage, under the high pressure in the fracture, the granular temporary plugging agent and fiber powder formed a temporary plugging filter cake. They were continuously compacted and the structure became tighter, leaving the fluid channel in the artificial fracture completely blocked.

Because of the high temperature during the temporary plugging process of artificial fractures, the performance of the temporary plugging agent changed across the four stages. Fig. 8(a) shows the distribution of the temporary plugging agent in the fracture after complete plugging at 50 °C. We observe that the temporary plugging agent was basically all in the front end of the fracture and the middle and back sections of the fracture were completely discharged. The distribution distance of the temporary plugging agent in the fracture is only 6 mm. Fig. 8(b) and (c) show the distribution of temporary plugging agents in artificial fractures at 100 and 150 °C, respectively. Compared with the distribution at 50 °C, the distributions at 100 and 150 °C show that the temporary plugging agents gradually formed in the middle and back sections of the fracture with the flow of the carrier fluid. After plugging, the distribution distance of the temporary plugging agent in the fracture increased significantly, as shown in Table 3. The main reason for this increase is that the temperature rose and it became relatively difficult to bridge the particles in the initial bridging stage. The particles gradually flowed forward in the fractures, and some particles formed bridges in the middle and back sections of the fractures. After entering the plugging stage, the fiber powder agglomerates were captured in the middle and back sections, causing the distribution distance of the temporary plugging agent

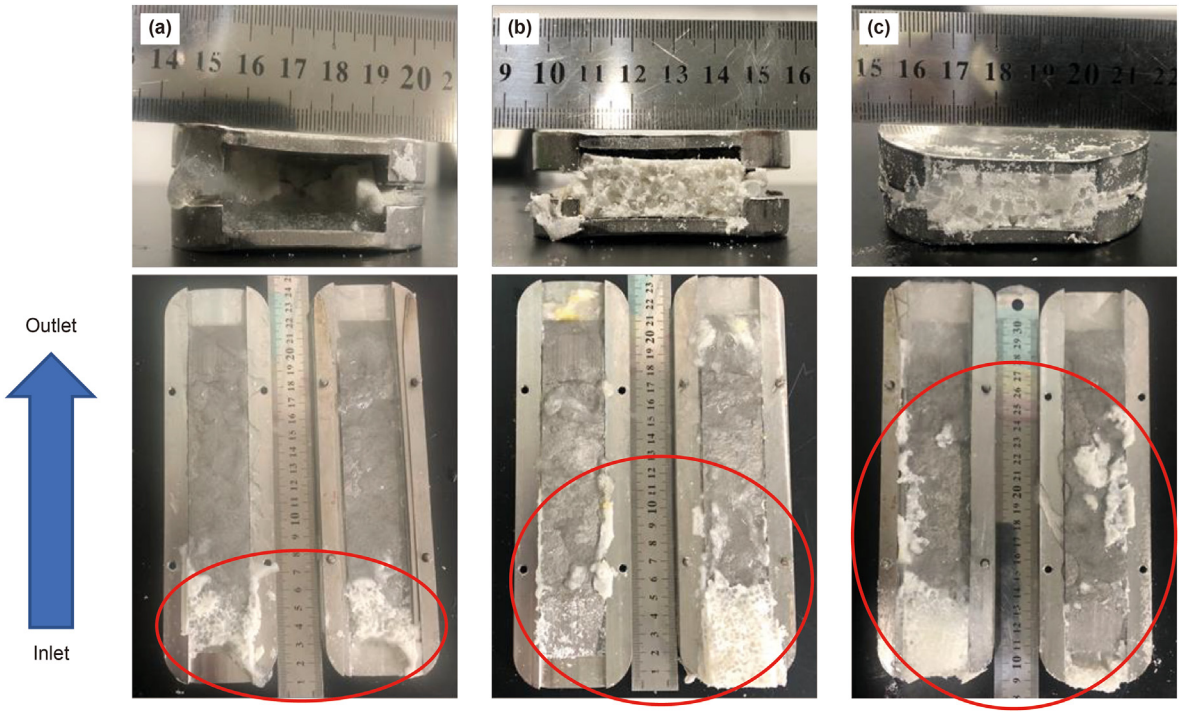

Fig. 8. Distribution of temporary plugging agent in fractures after the fractures are completely plugged under different temperature conditions. (**a**) 50 °C; (**b**) 100 °C; and (**c**) 150 °C.

Table 3
Distribution distance of temporary plugging agent in fractures under different temperature conditions.

Temperature, °C	Distribution distance of temporary plugging agent, cm
50	6
100	10
150	14

in the fracture to increase under high-temperature conditions. Thus, the results showed that particle bridging was difficult and fiber powder agglomerates had a hard time forming under high temperature.

(2) Injection pressure response

To study the effect of high temperature on the pressure response in a fracture and compare the results with room temperature (25 °C), we analyzed pressure changes in the artificial fracture during the temporary plugging process at the temperatures of 25, 50, 100, and 150 °C, respectively. As shown in Fig. 9, as the temperature increased, the number of pressure fluctuations increased significantly. The main reason for the increase of fluctuations is that the viscosity of the temporary plugging agent decreased at high temperature and the particles were difficult to bridge, making it difficult to form fiber powder agglomerates. Although the fiber powder agglomerates have formed a plugging section, the agglomerates could not withstand the high pressure in the fracture due to the unstable bridging structure. As a result, part of the granular temporary plugging agent and fiber powder were discharged with the carrier fluid to break through the blockage.

Also, we found that the number of plugging breakthroughs depended on the pressure fluctuations. Fig. 10 shows the change in the number of plugging breakthroughs at different temperatures. We observed that at room temperature, the temporary plugging agent in the fracture broke through once and then completely plugged the fracture. When the agent broke through in this state, the pressure in the fracture only reached 1.18 MPa. The pressure rapidly increased after a brief drop, and the temporary plugging agent formed a complete plug. At 50 °C, the number of plugging breakthroughs increased to five, and the pressure in the fracture was often higher than 1 MPa. When the temperature rose to 150 °C,

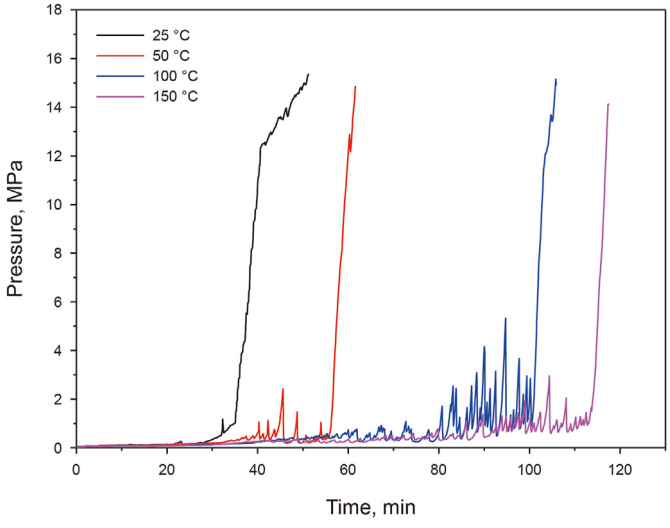

Fig. 9. Variations in fracture pressure during temporary plugging at different temperatures.

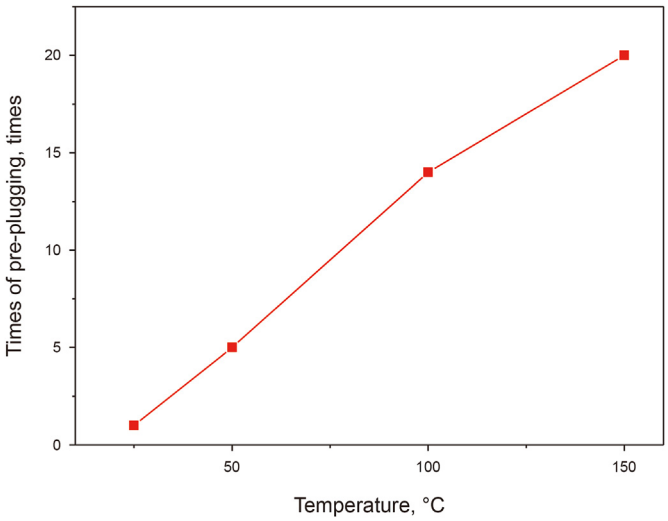

Fig. 10. Breakthrough plugging pressure times at different temperatures.

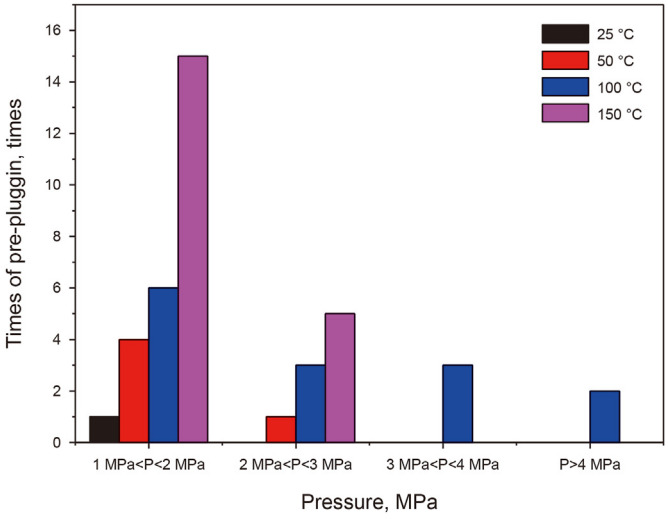

Fig. 11. Distribution of pressure fluctuations in fractures at different temperatures.

the fracture was completely sealed after 20 plugging breakthroughs and the pressure fluctuation frequency in the fracture was significantly different from that at the temperature of 100 °C. At 150 °C, during the plugging breakthrough process, the pressure fluctuations in the fracture mostly occurred in the range of 1–2 MPa, while at 100 °C, the pressure fluctuations were concentrated in the range of 2–3 MPa.

To analyze the pressure fluctuation range in the fracture, we counted the number of breakthrough pressures under different temperature and pressure conditions, as shown in Fig. 11. The pressure fluctuation is divided into four sections: 1–2, 2–3, 3–4 MPa and greater than 4 MPa. As the injection time increases, the injection pressure becomes higher. In the pressure fluctuation stage, under different temperature conditions, the breakthrough pressure was mainly distributed in the range of 1–3 MPa. The number of breakthrough pressures in the range of 1–2 MPa increased with increasing temperature. As the temperature increased from 50 to 150 °C, 15 pressure changes occurred, with the number of pressure changes nearly four times that at 50 °C. We observe that in the case of a plugging breakthrough, it was rare that the pressure in the fracture was greater than 4 MPa; indeed, the

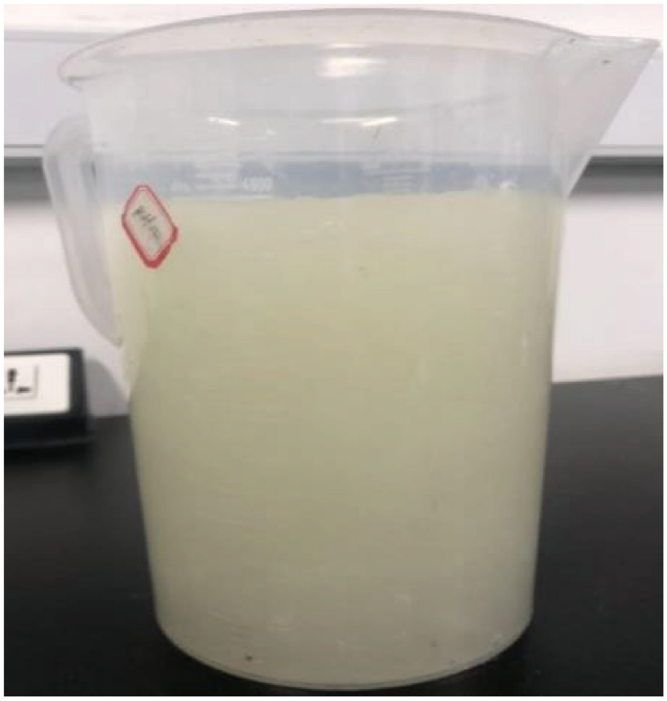

Fig. 12. Temporary plugging agent discharge during temporary plugging.

plugging breakthrough pressure was below 4 MPa in most cases. Then the plugging process entered the complete blocking stage and the pressure rose rapidly.

Under high pressure, the temporary plugging agent particles and fiber powder were discharged with the carrier fluid, breaking the blockage, and increasing the discharge volume. When the temperature rose by 100 °C, the drainage volume of the temporary plugging agent increased threefold. As shown in Fig. 12, the amount of temporary plugging agent discharged at 150 °C before complete plugging was 4500 mL.

(3) Plugging time

The rheology of the temporary plugging agent in the artificial fracture changed due to the increase of temperature. In particular, the time required for the initial bridging stage of the particles and the plugging stage of the particle-captured fiber powder agglomerates in the temporary plugging process gradually increased with the increase in temperature. To explore the effect of high temperature on the time required for temporary plugging, we collected data on the length of plugging time at different temperatures, as shown in Fig. 13. With an increase in temperature, the time required for fracture plugging increased gradually. Under normal temperature, the pressure in the fracture rose after one fluctuation and the time to form a complete blockage was only 51.2 min. When the temperature rose to 50 °C, the time required for plugging increased to 61.6 min. When the temperature was increased by 100 °C, the complete plugging time increased by 90.7%, and plugging was not completed until 117.5 min had passed.

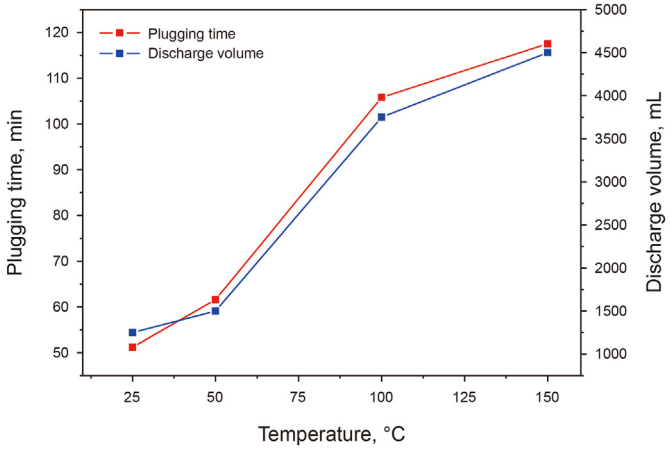

Fig. 13. Variations in plugging time and drainage volume of temporary plugging agent in fractures at different temperatures.

4.2. Effect of injection rate on temporary plugging characteristics

During the process of temporary plugging, it is necessary to change the injection rate according to the actual conditions of the site so as to achieve a better plugging effect. The injection rate of the temporary plugging agent is an important factor affecting the success of temporary plugging in fractures. In this section, we describe temporary plugging experiments in artificial fractures under the high temperature of 100 °C at different injection rates. These experiments capture the influence of injection rate on the plugging effect.

(1) Pressure response

Fig. 14 shows the pressure changes in the fracture under different injection rates during the temporary plugging process. Compared to a fracture under the normal temperature condition, the fracture under the 100 °C high-temperature condition showed obvious pressure fluctuations during the temporary plugging process. As the injection rate increases, the number of pressure fluctuations in the fracture increased significantly. When the injection rate was 30 mL/min, the number of pressure fluctuations in the slit was only 8. In contrast, as the injection rate increased to 50 mL/min, there were 15 pressure fluctuations in the fracture during the temporary plugging process. When the blocking reached the necessary strength corresponding to the fracture morphology, the fracture could bear a large range of pressure values. At this point, the temporary plugging process inside the artificial fracture entered the plugging stage formed by particle-captured fiber powder agglomerates.

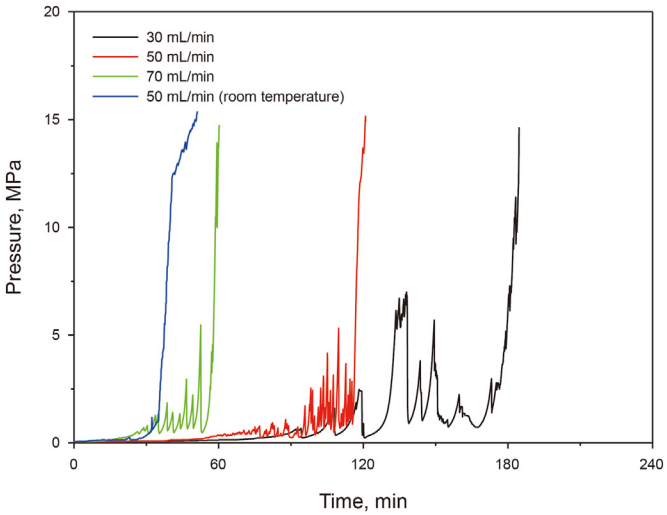

Fig. 14. Variations in pressure during temporary plugging at different injection rates.

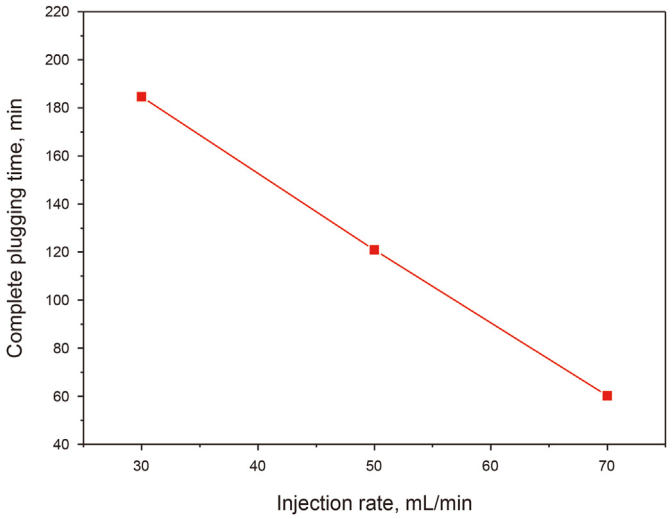

Fig. 15. Variations in amount of time required for complete plugging with temporary plugging agent at different injection rates.

(2) Plugging time

In the temporary plugging process, appropriate increases in the injection rate of the temporary plugging agent can shorten the time required for complete plugging in fractures. As shown in Fig. 15, when the injection rate was 30 mL/min, it took 184.6 min to form a complete plug. When the rate was increased to 50 mL/min, the temporary plugging agent in the fracture formed a complete plug by the 120.9-min marker. When the injection rate was increased to 70 mL/min, the time required for complete occlusion was further shortened to 60.2 min. As the injection rate increased under high temperature, the time required for complete plugging in the artificial fracture gradually decreased.

Furthermore, as the injection rate increased, the time required to reach a certain plugging strength gradually shortened. When the mechanical strength of the sealing zone was such that the plugging position in the fracture could withstand the >5 MPa pressure in the fracture, it took 133.1 min under the injection rate of 30 mL/min. At the injection rate of 70 mL/min, however, it only took 52.5 min, which was 60.5% shorter.

(3) Discharge volume

In the temporary plugging process, the amount of temporary plugging agent drainage is significantly affected by changes in the injection rate. Temporary plugging agent drainage mainly occurs before the fracture is completely plugged. As shown in Fig. 16, when the injection rate was 50 mL/min, the drainage volume of the temporary plugging agent was the largest at 3750 mL. When the injection rate was increased to 70 mL/min, the drainage volume decreased by 20%. As the injection rate of the temporary plugging agent increased, the time required for complete plugging of the artificial fracture decreased. The time required for the temporary plugging agent to be discharged through the outlet of the artificial fracture was correspondingly shortened, which in turn reduced the discharge volume to a certain extent. However, when the injection rate was 30 mL/min, it took a long time for complete plugging, and the drainage volume of the temporary plugging agent was less than 50 mL/min. The relatively slow injection rate of the temporary plugging agent may have caused the temporary plugging agent to drain slowly and the liquid discharge volume to be small in the lengthy incomplete plugging stage.

4.3. Effect of fracture width on temporary plugging characteristics

Given the strong in-situ stress anisotropy of hot dry rock reservoirs, fractures with different widths are likely to be generated in the process of hydraulic fracturing. These generated fractures stimulate reservoir fractures. The different fracture widths of the reservoir fractures affect the temporary plugging properties of the temporary plugging agent. In this section, we describe temporary plugging experiments in the artificial fracture under the high temperature of 100 °C and at different fracture widths. These experiments reveal the effect of artificial fracture width under high temperature on the plugging effect of the temporary plugging agent.

(1) Pressure response

Fig. 17 shows the change in pressure during temporary plugging under different fracture widths. When the fracture width was 4 mm, the time required for the formation of effective pressure suppression in the fracture under high temperature was 2.7 times

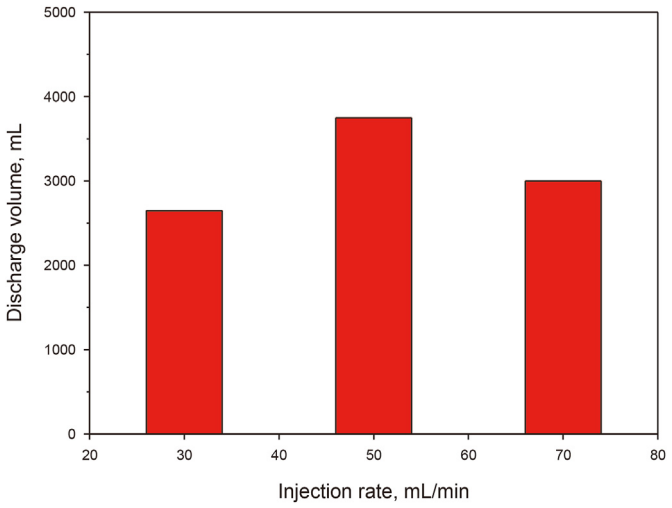

Fig. 16. Discharge volume of temporary plugging agent during temporary plugging process under different injection and discharge rates.

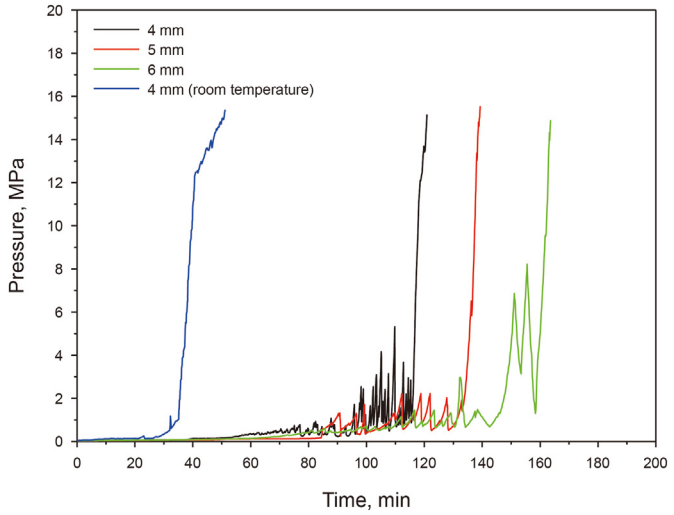

Fig. 17. Variations in pressure during temporary plugging with different fracture widths.

greater than it was under the normal temperature state. Compared with the normal temperature state, in the high-temperature state, there was an obvious fracture pressure fluctuation stage during the temporary plugging process with different fracture widths. Different fracture widths caused significant differences in the pressure fluctuation states. Under a fracture width of 4 mm, the pressure fluctuation in the fracture was mainly distributed in the range of 2–4 MPa. When the fracture width increased, the pressure fluctuation range decreased significantly. Under a fracture width of 5 or 6 mm, the pressure fluctuation in the fracture was mainly concentrated in the range of 1–2 MPa; that is, there were no large pressure changes. However, when the fracture width was 6 mm, there were two large pressure fluctuations in the later stage of the temporary plugging of the pressure in the fracture. The main reasons for this are twofold. First, in this state, the fracture width was close to twice the particle diameter. Second, the rough fracture wall in the early stage of plugging hindered the forward transport of particles, causing the particles to gradually form bridges in the fractures. However, due to the relatively small diameter of the particles, the bridging in the joint was unstable. When, under high pressure, the bridging particles begin to capture the fiber powder agglomerates, bridging instability is likely to occur. This bridging instability causes the phenomenon of breakthrough and blockage, and the pressure in the fracture drops. With the continuous accumulation of particles and fibrous powder viscous bodies in the fracture to bridge and seal, the pressure in the fracture continues to rise until it is completely blocked.

(2) Distribution of temporary plugging agent in fractures

Fig. 18 shows the distribution distance of the temporary plugging agent in the fracture under different fracture widths. As the fracture width increased, the distribution distance of the temporary plugging agent in the fracture gradually increased. When the fracture width was 4 mm, due to the limitation of the fracture width, it was difficult for the temporary plugging agent particles to be transported inside the fracture once they had entered the fracture. Immediately after bridging and plugging, the artificial fracture was completely plugged, and the temporary plugging agent was mainly distributed at the fracture inlet. As shown in Fig. 18(b), when the fracture width was increased to 5 mm, the temporary plugging agent distribution extended to the inside of the fracture and complete plugging was formed in the middle of the fracture. At this time, the particles of the temporary plugging agent in the fracture were distributed in a single layer. When the temporary plugging experiment was carried out under a fracture width of 6 mm, after the fracture was completely plugged, the temporary plugging agent filled the fracture area, as shown in Fig. 18(c). Compared with a fracture width of 5 mm, a fracture width of 6 mm meant that the temporary plugging agent particles were obviously stacked in the fracture and the particles were distributed in two layers in many plugging areas.

Fig. 19 shows the temporarily blocked body obtained by computed tomography (CT) scan. With an increase in fracture width, the plugging distance of the temporary plugging agent in the fracture gradually increases. When the fracture width is small, the plugging is mainly concentrated at the front end of the fracture.

The increase in fracture width increases the transport distance of the temporary plugging agent inside the fracture to a certain extent, which in turn prolongs the time required for complete plugging. In this study's experiments, 3 mm particles were used to successfully plug the rough cracks with a width of 6 mm. The results indicate that under certain experimental conditions, the temporary plugging agent particles combined with fiber powder were able to effectively plug the fractures whose width was twice the particle diameter. However, the scope of this paper is limited to temporary plugging experiments carried out on a set of fracture models. For fracture plugging under different rough conditions, further research is necessary.

(3) Rheological properties of the carrier fluid at different temperature

Using a high-temperature and high-pressure rheometer, we carried out experimental research on the rheological properties of the temporary plugging agent carrier fluid at temperatures of 87 and 120 °C, as shown in Fig. 20(a) and (b). It can be seen that when the temperature is 87 °C and the shearing time is 170 s^{-1} for 67 min, the final viscosity is 264.7 mPa·s, among which: the viscosity of continuous shearing for 0–30 min is 928–259.5 mPa·s; the viscosity of continuous shearing for 30–67 min is 264.7–259.5 mPa·s. When the temperature is 120 °C and the shearing time is 170 s^{-1} for 90 min, the final viscosity is about 100 mPa·s. Therefore, as the temperature rises, the viscosity of the carrier fluid of the temporary plugging agent decreases, the rheology of the fluid becomes worse, and it is more difficult to carry the temporary plugging agent into the fracture, and the difficulty of plugging also increases.

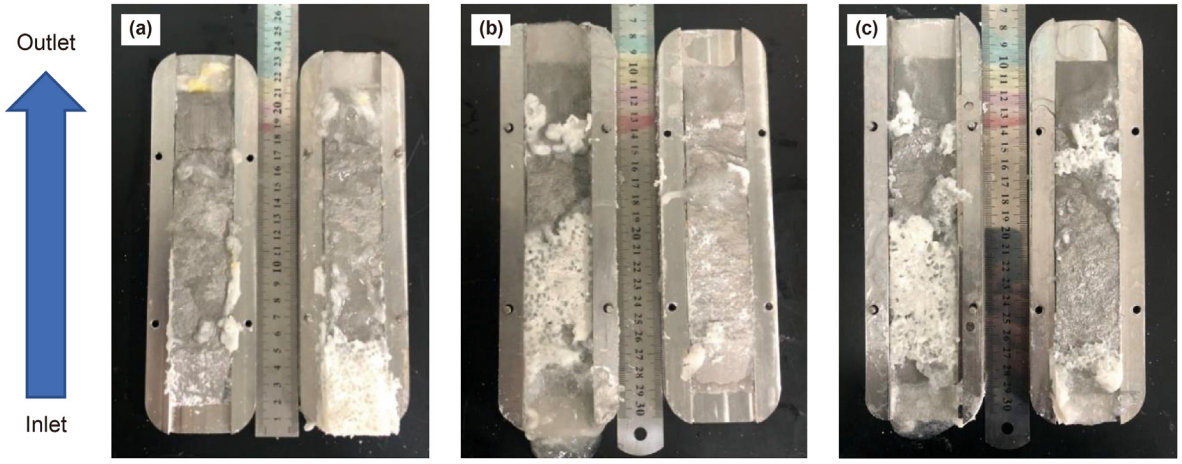

Fig. 18. Distribution of temporary plugging agent in fractures with different fracture widths. (**a**) 4 mm; (**b**) 5 mm; and (**c**) 6 mm.

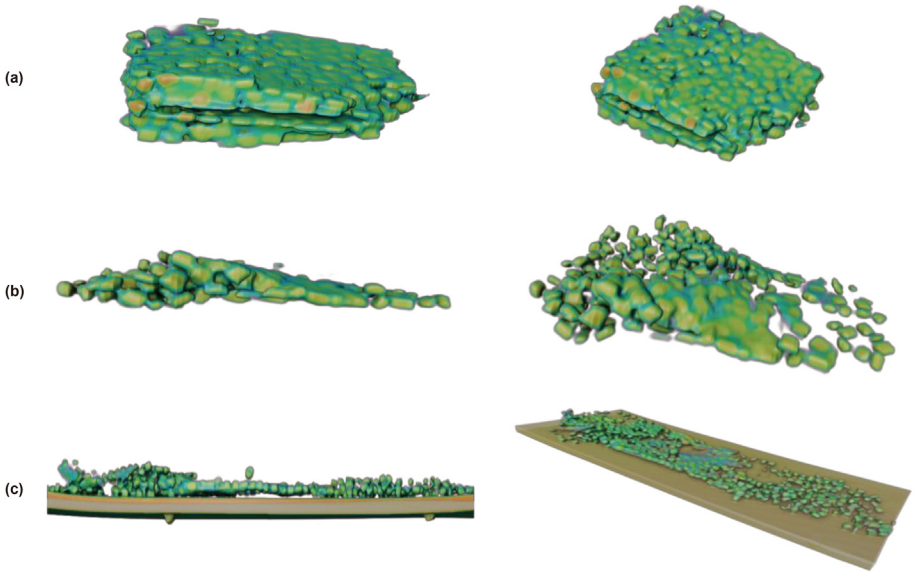

Fig. 19. Temporary block diagram obtained by CT scan. (**a**) 4 mm; (**b**) 5 mm; and (**c**) 6 mm.

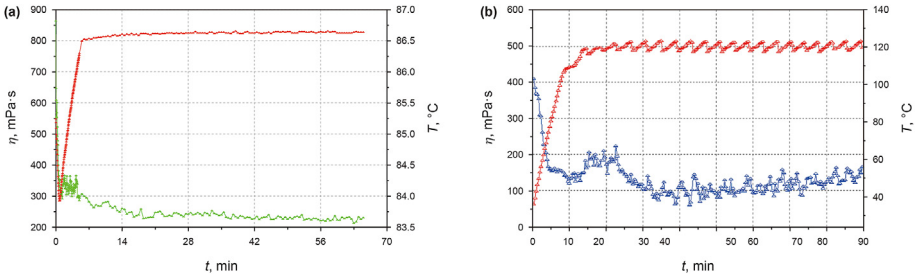

Fig. 20. Rheological properties of the carrier fluid at different temperature. (**a**) 87 °C; and (**b**) 120 °C.

5. Conclusion

In this paper, an artificial fracture model of hot dry rock was prepared by means of a rock expansion-induced cracking experiment and 3D printing technology; an improved experimental system for evaluating temporary plugging performance at high temperature was established. On this basis, we formulated and carried out an experimental scheme for the temporary plugging of artificial fractures under high temperature. The effects of high temperature, injection rate, fracture width, and other factors on the plugging process of the temporary plugging agent, the pressure response in the fracture, the plugging time, and the distribution distance of the temporary plugging agent in the fracture were analyzed. The main conclusions are as follows:

(1) The process of temporarily plugging artificial fractures in hot dry rock has four main stages: the initial stage of temporary plugging, the stage of particle bridging, the stage of plugging formation, and the stage of dense plugging. During these four stages, the distribution of the temporary plugging agent in the fracture changes with the temperature. As the temperature increases by 50 °C, the distribution distance of the temporary plugging agent in the fracture increases by 66.7%.

(2) Under high-temperature conditions, there exist apparent pressure fluctuations during the temporary plugging of artificial fractures. As the temperature increases, the number of pressure fluctuations increases. Also, under high-pressure conditions, there is an obvious difference in the number of plugging breakthroughs and pressure fluctuations. When the temperature rose to 150 °C, the fractures were completely blocked after 20 plugging breakthroughs. As the temperature increased, the time required for fracture plugging increased gradually. When the temperature increased by 100 °C, the time required for complete plugging increased by 90.7%.

(3) Under high-temperature conditions, as the injection rate increases, the number of pressure fluctuations in artificial fractures increases significantly. When the injection rate increased to 50 mL/min, there were 15 pressure fluctuations in fractures during the temporary plugging process. The time required for the complete plugging of the fractures generally showed a downward linear trend as the injection rate increased. Appropriately increasing the injection rate of the temporary plugging agent shortened the time required for the complete plugging of artificial fractures to a certain extent.

(4) As the fracture width increases, the distribution distance of the temporary plugging agent in the fracture gradually increases. After the fracture with a width of 6 mm was completely blocked, the temporary plugging agent filled the whole fracture. The pressure fluctuation states caused by different fracture widths were significantly different. Under certain experimental conditions, temporary plugging agent particles combined with fiber powder could effectively plug cracks whose width is twice the particle diameter.

Data availability

Datasets related to this article can be found by connecting with the corresponding author.

Declaration of competing interest

The authors declare that they have no known competing financial interests or personal relationships that could have appeared to influence the work reported in this paper.

Acknowledgments

This work was supported financially by the Beijing Natural Science Foundation Project (No. 3222030), the National Natural Science Foundation of China (No. 51936001, No. 52274002 and No. 52192622), the PetroChina Science and Technology Innovation Foundation Project (2021DQ02–0201), and Award Cultivation Foundation from Beijing Institute of Petrochemical Technology (No. BIPTACF-002).

References

Allison, D., Curry, S., Todd, B., 2011. Restimulation of wells using biodegradable particulates as temporary diverting agents. In: Presented at the Canadian Unconventional Resources Conference, OnePetro. https://doi.org/10.2118/149221-MS.

Alsaba, M., Al Dushaishi, M.F., Nygaard, R., Nes, O.M., Saasen, A., 2017. Updated criterion to select particle size distribution of lost circulation materials for an effective fracture sealing. J. Pet. Sci. Eng. 149, 641–648. https://doi.org/10.1016/j.petrol.2016.10.027.

Alsaba, M., Nygaard, R., Saasen, A., Nes, O.M., 2014. Lost circulation materials capability of sealing wide fractures. In: Presented at the SPE Deepwater Drilling and Completions Conference, OnePetro. https://doi.org/10.2118/170285-MS.

Calçada, L.A., Duque Neto, O.A., Magalhães, S.C., Scheid, C.M., Borges Filho, M.N., Waldmann, A.T.A., 2015. Evaluation of suspension flow and particulate materials for control of fluid losses in drilling operation. J. Pet. Sci. Eng. 131, 1–10. https://doi.org/10.1016/j.petrol.2015.04.007.

Droger, N., Eliseeva, K., Todd, L., Ellis, C., Salih, O., Silko, N., Fu, D., Meyer, A., Bermudez, R., 2014. Degradable fiber pill for lost circulation in fractured reservoir sections. In: Presented at the IADC/SPE Drilling Conference and Exhibition, OnePetro. https://doi.org/10.2118/168024-MS.

Evans, K.F., Cornet, F.H., Hashida, T., Hayashi, K., Ito, T., Matsuki, K., Wallroth, T., 1999. Stress and rock mechanics issues of relevance to HDR/HWR engineered geothermal systems: review of developments during the past 15 years. Geothermics 28, 455–474. https://doi.org/10.1016/S0375-6505(99)00023-1.

Fehler, M.C., 1989. Stress control of seismicity patterns observed during hydraulic fracturing experiments at the Fenton Hill hot dry rock geothermal energy site, New Mexico. Int. J. Rock Mech. Min. Sci. Geomech. Abstr. 26, 211–219. https://doi.org/10.1016/0148-9062(89)91971-2.

Geothermal Energy, 2013. Utilization and technology. Routledge. https://doi.org/10.4324/9781315065786.

Ghassemi, A., 2012. A review of some rock mechanics issues in geothermal reservoir development. Geotech. Geol. Eng. 30, 647–664. https://doi.org/10.1007/s10706-012-9508-3.

Kumari, W.G.P., Ranjith, P.G., Perera, M.S.A., Li, X., Li, L.H., Chen, B.K., Isaka, B.L.A., De Silva, V.R.S., 2018. Hydraulic fracturing under high temperature and pressure conditions with micro CT applications: geothermal energy from hot dry rocks. Fuel 230, 138–154. https://doi.org/10.1016/j.fuel.2018.05.040.

Li, B., Zhou, F., Yuan, L., Li, H., Cheng, J., Tan, Y., Zhang, Y., Xian, B., Fan, W., 2019. Experimental investigation on the fracture diverting mechanism and plugging efficiency using 3D printing fractures. In: Presented at the 53rd U.S. Rock Mechanics/Geomechanics Symposium, OnePetro.

Li, J., Yang, H., Qiao, Y., Fan, Z., Chen, W., Jiang, H., 2018. Laboratory evaluations of fiber-based treatment for in-depth profile control. J. Pet. Sci. Eng. 171, 271–288. https://doi.org/10.1016/j.petrol.2018.07.060.

Liang, T., Zhou, F., Shi, Y., Liu, X., Wang, R., Li, B., Li, X., 2018. Evaluation and optimization of degradable-fiber-assisted slurry for fracturing thick and tight formation with high stress. J. Pet. Sci. Eng. 165, 81–89. https://doi.org/10.1016/j.petrol.2018.02.010.

Liu, J., 2017. Study on Optimizing the Fiber-Particle Composite Temporary Plugging and Diverting Technique. China University of Petroleum-Beijing, Beijing, China.

Mansour, A.K., Taleghani, A.D., Li, G., 2017. Smart lost circulation materials for wellbore strengthening. In: Presented at the 51st U.S. Rock Mechanics/Geomechanics Symposium, OnePetro.

Potapenko, D.I., Tinkham, S.K., Lecerf, B., Fredd, C.N., Samuelson, M.L., Gillard, M.R., Le Calvez, J.H., Daniels, J.L., 2009. Barnett shale refracture stimulations using a novel diversion technique. In: Presented at the SPE Hydraulic Fracturing Technology Conference, OnePetro. https://doi.org/10.2118/119636-MS.

Shi, Y., Zhou, F., Yang, X., Liu, X., Lian, S., Li, X., 2013. Laboratory study and field application of fiber-based fracture reorientation technology. In: Presented at the International Petroleum Technology Conference, OnePetro. https://doi.org/10.2523/IPTC-16736-MS.

Smith, C.L., Anderson, J.L., Roberts, P.G., 1969. New diverting techniques for acidizing and fracturing. In: Presented at the SPE California Regional Meeting, OnePetro. https://doi.org/10.2118/2751-MS.

Van Domelen, S.M., 2017. A practical guide to modern diversion technology. In: Presented at the SPE Oklahoma City Oil and Gas Symposium, OnePetro. https://doi.org/10.2118/185120-MS.

Wang, D., 2017. Diverting Mechanism and its Law of Temporary Plugging in Hydraulic Fracturing. China University of Petroleum-Beijing, Beijing, China.

Wang, D., Dong, Y., Sun, D., Yu, B., 2020. A three-dimensional numerical study of hydraulic fracturing with degradable diverting materials via CZM-based FEM. Eng. Fract. Mech. 237, 107251. https://doi.org/10.1016/j.engfracmech.2020.107251.

Wang, D., Qin, H., Zheng, C., Sun, D., Yu, B., 2023. Transport mechanism of temporary plugging agent in complex fractures of hot dry rock: a numerical study. Geothermics 111, 102714. https://doi.org/10.1016/j.geothermics.

Wang, D., Zhou, F., Ding, W., Ge, H., Jia, X., Shi, Y., Wang, X., Yan, X., 2015a. A numerical simulation study of fracture reorientation with a degradable fiber-diverting agent. J. Nat. Gas Sci. Eng. 25, 215–225. https://doi.org/10.1016/j.jngse.2015.05.002.

Wang, D., Zhou, F., Dong, Y., Sun, D., Yu, B., 2021. Experimental investigation of thermal effect on fracability index of geothermal reservoirs. Nat. Resour. Res. 30, 273–288. https://doi.org/10.1007/s11053-020-09733-0.

Wang, D., Zhou, F., Ge, H., Shi, Y., Yi, X., Xiong, C., Liu, X., Wu, Y., Li, Y., 2015b. An experimental study on the mechanism of degradable fiber-assisted diverting fracturing and its influencing factors. J. Nat. Gas Sci. Eng. 27, 260–273. https://doi.org/10.1016/j.jngse.2015.08.062.

Xue, S., Zhang, Z., Wu, G., Wang, Y., Wu, J., Xu, J., 2015. Application of a novel temporary blocking agent in refracturing. In: Presented at the SPE Asia Pacific Unconventional Resources Conference and Exhibition, OnePetro. https://doi.org/10.2118/176900-MS.

Yuan, L., Zhou, F., Li, B., Gao, J., Yang, X., Cheng, J., Wang, J., 2020. Experimental study on the effect of fracture surface morphology on plugging efficiency during temporary plugging and diverting fracturing. J. Nat. Gas Sci. Eng. 81, 103459. https://doi.org/10.1016/j.jngse.2020.103459.

Zhang, L., Zhou, F., Mou, J., Pournik, M., Tao, S., Wang, D., Wang, Y., 2019. Large-scale true tri-axial fracturing experimental investigation on diversion behavior of fiber using 3D printing model of rock formation. J. Pet. Sci. Eng. 181, 106171. https://doi.org/10.1016/j.petrol.2019.06.035.

Zhang, Y., Zhao, G.F., 2019. A global review of deep geothermal energy exploration: from a view of rock mechanics and engineering. Geomech. Geophys. Geo-Energy Geo-Resour. 6, 4. https://doi.org/10.1007/s40948-019-00126-z.

Zhou, F., Liu, Y., Liu, X., Xiong, C., Yang, X., Jia, X., Li, X., Wang, D., Zhang, F., Shi, H., Lian, Y., Tao, S., Qian, C., 2009. Case study:ym204 obtained high petroleum production by acid fracture treatment combining fluid diversion and fracture reorientation. In: Presented at the 8th European Formation Damage Conference, OnePetro. https://doi.org/10.2118/121827-MS.

Zhou, H., Wu, X., Song, Z., Zheng, B., Zhang, K., 2022. A review on mechanism and adaptive materials of temporary plugging agent for chemical diverting fracturing. J. Pet. Sci. Eng. 212, 110256. https://doi.org/10.1016/j.petrol.2022.110256.

Zheng, C., Wang, D., Shen, B., Wang, Q., Liu, X., Sun, D., Yu, B., 2023. An experimental study of the temporary plugging mechanisms of rough fractures in hot dry rocks under a high temperature. Powder Technology 427, 118687. https://doi.org/10.1016/j.powtec.2023.118687.